HHS Public Access

Author manuscript

Nat Med. Author manuscript; available in PMC 2010 January 01.

Published in final edited form as:

Nat Med. 2009 July ; 15(7): 757–765. doi:10.1038/nm.1979.

TGF-β1-induced Migration of Bone Mesenchymal Stem Cells Couples Bone Resorption and Formation

Yi Tang[1,7], **Xiangwei Wu**[1,2,3,7], **Weiqi Lei**[1], **Lijuan Pang**[1,4], **Chao Wan**[1], **Zhenqi Shi**[1], **Ling Zhao**[1], **Timothy R. Nagy**[5], **Xinyu Peng**[3], **Junbo Hu**[2], **Xu Feng**[1], **Wim Van Hul**[6], **Mei Wan**[1], and **Xu Cao**[1]

[1] Department of Pathology, University of Alabama at Birmingham, Birmingham, Alabama 35294, USA

[2] Tongji Hospital, Tongji Medical College, Huazhong University of Science and Technology, Wuhan, Hubei 430030, China

[3] The First Affiliated Hospital, School of Medicine, Shihezi University, Shihezi, Xinjiang 832008, China

[4] Department of Pathology, School of Medicine, Shihezi University, Shihezi, Xinjiang 832002, China

[5] Departments of Nutrition Sciences, University of Alabama at Birmingham, Birmingham, Alabama 35294, USA

[6] Department of Medical Genetics, University of Antwerp, Antwerp, Belgium

SUMMARY

Bone remodeling depends on the precise coordination of bone resorption and subsequent bone formation. Disturbances of this process are associated with skeletal diseases, such as Camurati-Engelmann disease (CED). We show using *in vitro* and animal models that active TGF-β1 released during bone resorption coordinates bone formation by inducing migration of bone marrow stromal cells, also known as bone mesenchymal stem cells (BMSCs) to the bone resorptive sites and that this process is mediated through SMAD signaling pathway. Analysis of a mouse model carrying a CED-derived *TGF-β1* mutation, which exhibits the typical progressive diaphyseal dysplasia with tibial fractures, we found high levels of active TGF-β1 in the bone marrow. Treatment with a TGF-β type I receptor inhibitor partially rescued the uncoupled bone remodeling and prevented the fractures. Thus, as TGF-β1 functions to couple bone resorption and formation, modulation of TGF-β1 activity could be an effective treatment for the bone remodeling diseases.

Corresponding author: Xu Cao, 1670 University Blvd., VH G003, Birmingham, AL 35294-0019, Telephone: (205) 934-0162, Fax: (205) 934-1775, E-mail: cao@uab.edu.

[7]These authors contributed equally to this work.

Note: More details of experimental procedures are shown in supplementary Information.

INTRODUCTION

In the adult skeleton, bone is continuously being formed and resorbed1. This bone remodeling process is accomplished by a precise coordination of the activities of two cell types: osteoblasts, which deposit the calcified bone matrix, and osteoclasts, which resorb bone2,3. Bone resorption and formation do not occur along the bone surface at random. Rather, they occur at specific anatomical sites and follow a well-defined sequence of events, which is known as the bone remodeling cycle4. Disturbances of the bone remodeling process are often associated with skeletal diseases3, including CED, which is an inherited skeleton remodeling disorder, characterized by a fusiform thickening of the diaphyses of the long bones and skull5–7.

Coupling of bone resorption and formation is believed through release of a factor, or factors, from the bone matrix during osteoclastic bone resorption that directs migration of BMSCs to the bone resorptive surfaces8–12. The osteoclastic bone resorptive sites contain a number of soluble osteotropic factors, including transforming growth factor-β1 (TGF-β1)13–15. TGF-β1 is one of the most abundant cytokines in the bone matrix (200 μg kg^{-1})15–17. TGF-β1 is synthesized as a large precursor molecule, which is cleaved into active TGF-β1 and latency-associated protein (LAP). The LAP remains non-covalently linked to active TGF-β1, masking the receptor-binding domains of the active TGF-β1 and rendering it inactive18,19. TGF-β1 is thus secreted and deposited in the bone matrix as an inactive, latent complex20,21. TGF-β1 has been shown to regulate proliferation and differentiation of osteoprogenitors, but the exact function of TGF-β1 in bone is unclear22–25. Mapping of the chromosomal region associated with CED has identified *TGF-β1* as a candidate gene and approximately ten different *TGF-β1* mutations have been identified in samples from CED families5,6. In twenty four CED families with *TGF-β1* mutations, twenty two individuals have a mutation located in the region encoding LAP; however, no mutations were found in the domain encoding the active TGF-β1-peptide5,6,26. Moreover, active TGF-β1 was readily released upon over-expression of the CED *TGF-β1* mutants in cultured cells27,28.

BMSCs have been found to differentiate into a variety of cell types, including osteoblasts, chondrocytes, and adipocytes, depending on the stimulatory microenvironment29,30. BMSCs that are identified by the expression of STRO-131,32 or CD14633 in humans and expression of CD29 and Sca-1 in mice34,35 have been characterized in terms of their potential for differentiation into osteoblasts and are widely used as experimental models of bone remodeling, fracture healing, and bone regeneration, although there is no unique marker specific for the lineage of osteogenic BMSCs29,30,36–39. Here, we demonstrate that the active TGF-β1 released in response to osteoclastic bone resorption induces migration of human and mouse osteogenic BMSCs through SMAD signaling in different animal models. High levels of active TGF-β1 were found in the bone marrow microenvironment in CED mice. Treatment with TGF-β type I receptor (TβRI) inhibitor partially rescued bone defects in the CED mice. Thus, TGF-β1 functions as a primary factor for recruitment of BMSCs to the bone remodeling surfaces in the coupling process.

RESULTS

TGF-β1 from bone resorption induces migration of BMSCs

We reasoned that the potential factor(s) should be released into the media when mature and functional osteoclasts are cultured with bone slices *in vitro* and that the bone resorption-conditioned media (BRCM) could then be tested for its effect on the migration of BMSCs. We first confirmed that on culture with macrophage colony-stimulating factor (M-CSF) and RANKL, the monocytes/macrophages differentiated into osteoclasts that exhibited a multi-nuclear morphology, tartrate-resistant acid phosphatase (TRAP) positive staining and bone resorption activity (Supplementary Fig. 1a). In the absence of RANKL, the precursors failed to differentiate into mature osteoclasts and did not exhibit bone resorption activity (Supplementary Fig. 1a). The effects of conditioned media on the migration of STRO-1^+ BMSCs (Supplementary Fig. 1b) purified from human bone marrow were examined using a Transwell assay in which the BMSCs were placed in the upper chamber and the conditioned media were placed in the lower chamber (Supplementary Fig. 1c). We found that the BRCM from mature osteoclasts cultured in the presence of bone slices induced significantly greater cell migration (Fig. 1a) than the control conditioned media, confirming that a factor(s) released during bone resorption can induce migration of BMSCs.

Many osteotropic factors are found in the bone matrix, including bone morphogenetic proteins (BMPs), platelet-derived growth factor (PDGF), and the insulin-like growth factors-I or -II (IGF-I or IGF-II), as well as the TGF-βs13,20,40. The recombinant forms of these factors have been shown to induce cell migration *in vitro*12,41. We found that addition of an antibody specific for TGF-β1 to the BRCM significantly inhibited the migration of human STRO-1^+ BMSCs, whereas antibodies specific for IGF-II or PDGF had a slight inhibitory effect and antibodies specific for TGF-β2, TGF-β3, IGF-I, or noggin, a BMP antagonist, had no detectable effects (Fig. 1b), indicating that TGF-β1 is a primary inducer of the migration of BMSCs in this assay.

High levels of active TGF-β1 were present in the conditioned media from osteoclasts prepared in the presence of bone slices as shown by ELISA (Fig. 1c) and western blot analysis (Fig. 1d). Taken together with the finding that active TGF-β1 was barely detectable in the conditioned media prepared in the absence of bone slices or in the other control conditioned media although inactive latent TGF-β1 was present, these data suggest that osteoclastic bone resorption is critical for the activation of TGF-β1. Depletion of TGF-β1 in the BRCM by immunoprecipitation with an antibody to TGF-β1 significantly compromised the ability of the BRCM to induce cell migration, and readdition of TGF-β1 to the depleted media restored its ability to induce cell migration in a concentration-dependent manner (Fig. 1e). Moreover, BRCM prepared using osteoclasts generated from precursors of normal mice and bone slices obtained from *Tgfb1* knockout (*Tgfb1*$^{-/-}$) mice, which contained barely detectable levels of active TGF-β1 (Fig. 1f), was significantly less effective in inducing migration of BMSCs than BRCM obtained from osteoclasts cultured with wild type (WT) bone (Fig. 1g). However, the reduction of cell migration associated with the use of BRCM prepared from cells and bone from the *Tgfb1*$^{-/-}$ mice was not as significant as the inhibition observed on addition of the TGF-β1 neutralizing antibody to the WT BRCM (Fig. 1b,g)

suggesting that in the absence of TGF-β1, other factors may be present in higher concentrations that partially support the migration of BMSCs in *Tgfb1*$^{-/-}$ mice. Taken together, these results indicate that active TGF-β1 released during osteoclastic bone resorption induces migration of BMSCs, at least under the conditions of this assay.

TGF-β1 is essential for bone remodeling in adult mice

We then determined the potential role of TGF-β1-induced migration of BMSCs using *Tgfb1*$^{-/-}$ mice. TGF-β1 has been shown to regulate proliferation of osteoprogenitors and to inhibit differentiation of osteoblasts *in vitro*23,42. The skeleton of *Tgfb1*$^{-/-}$ mice appears normal at one-month of age (prior to death due to organ failure associated with autoimmune disease43), and the mice exhibit depletion of preosteoblasts at the trabecular bone surfaces and the presence of osteoprogenitors in the middle of bone marrow44,45. To examine the potential involvement of TGF-β1 in the process of migration of BMSCs to the bone surface during bone remodeling in adult mice, we prevented the autoimmune disease, thus extending the life of the mice, by crossing the *Tgfb1*$^{-/-}$ mice with immunodeficient *Rag2*$^{-/-}$ mice46,47. Analysis of the one month-old *Tgfb1*$^{-/-}$ *Rag2*$^{-/-}$ mice confirmed that they did not exhibit significant differences in trabecular bone volume, thickness and separation as measured by μCT (Supplementary Fig. 2a–c), whereas, as compared to their WT littermates, the three month-old *Tgfb1*$^{-/-}$*Rag2*$^{-/-}$ mice exhibited a significant loss of trabecular bone volume and thickness, and greater trabecular bone separation (Fig. 2a–d). Histologic staining of femur sections also indicated that the trabecular bone was irregular and notably reduced (Fig. 2e and Supplementary Fig. 2d). Moreover, bone histomorphometric analyses revealed a significant reduction in osteoblasts but little change in the numbers of osteoclasts in the three month-old *Tgfb1*$^{-/-}$*Rag2*$^{-/-}$ mice as compared to their WT littermates (Fig. 2f,g). Furthermore, immunostaining of femur sections demonstrated that Runx2-positive osteoblasts were missing on trabecular bone surface of the three month-old *Tgfb1*$^{-/-}$*Rag2*$^{-/-}$ mice (Fig. 2h), suggesting a deficiency of osteoblasts on bone surfaces.

To examine the osteogenic potential of the BMSCs, whose misfunction may contribute to the bone loss in the adult *Tgfb1*$^{-/-}$*Rag2*$^{-/-}$ mice, suspensions of BMSCs isolated from the three month-old *Tgfb1*$^{-/-}$*Rag2*$^{-/-}$ mice or their WT littermates were plated at clonal density to obtain discrete colonies (colony forming unit-fibroblast [CFU-F]). The CFU-Fs were further induced in osteogenic media and assessed their alkaline phosphatase activity (colony forming unit-osteoblast [CFU-Ob]) and calcium deposition by Alizarin Red staining. The results indicated that the osteogenic potential of the BMSCs of the three month-old *Tgfb1*$^{-/-}$*Rag2*$^{-/-}$ mice was equivalent to the osteogenic potential of the BMSCs of their WT littermates (Fig. 2i,j). Considering that no bone defects are evident during prenatal development or the first month of postnatal growth of the *Tgfb1*$^{-/-}$ mice, these results indicate a potential role for TGF-β1 in the migration of BMSCs to the bone surfaces and in the coupling process during bone remodeling in the adult mice.

TGF-β1 induces migration of BMSCs to the remodeling sites

To examine whether TGF-β1 induces migration of BMSCs to the bone remodeling surface in mice, we injected the osteogenic BMSCs into the femur cavity of the *Tgfb1*$^{+/+}$*Rag2*$^{-/-}$ and *Tgfb1*$^{-/-}$*Rag2*$^{-/-}$ mice. Since there is no unique marker for BMSCs, mouse

$CD29^+Sca\text{-}1^+CD45^-CD11b^-$ BMSCs were isolated by fluorescence-activated cell sorting (FACS) from mouse BMSCs (Fig. 3a,b). 95% of the sorted cells were then confirmed to be osteogenic by analysis of formation of CFU-Ob colonies as detected by alkaline phosphatase activity (Fig. 3c), and the osteogenic potential was further confirmed by von Kossa and Alizarin Red staining (Fig. 3d). We also confirmed that the sorted BMSCs underwent BRCM-induced migration that was inhibited by the TβRI inhibitor (Fig. 3e). The BMSCs were then labeled with GFP using retrovirus and injected into the femur cavity of the $Tgfb1^{+/+}Rag2^{-/-}$ or $Tgfb1^{-/-}Rag2^{-/-}$ mice (Fig. 3f). The injected BMSCs were detected by immunostaining of the femur sections with an antibody against GFP one week or four weeks after injection (Fig. 3g). In the $Tgfb1^{+/+}Rag2^{-/-}$ mice, the GFP-positive BMSCs were largely found at the trabecular bone surface at one week after injection. At four weeks after injection, some of the GFP-positive BMSCs were embedded in the trabecular bone of these $Tgfb1^{+/+}Rag2^{-/-}$ mice, indicating osteoblastic differentiation of the injected BMSCs (Fig. 3g,h). In contrast, in the $Tgfb1^{-/-}Rag2^{-/-}$ mice the GFP-positive BMSCs were dispersed in the bone marrow and most of the BMSCs were not found at the bone surface at one week or four weeks after injection (Fig. 3g,h).

In a similar *in vivo* migration experiment, human $STRO\text{-}1^+CD45^-$ BMSCs were injected into the femur cavity of the immuno-deficient $Tgfb1^{+/+}Rag2^{-/-}$ and $Tgfb1^{-/-}Rag2^{-/-}$ mice. The injected BMSCs were detected by immunostaining of the femur sections with antibodies against human leukocyte antigen A (HLA-A) and RUNX2 to track migration and osteoblastic differentiation. In the $Tgfb1^{+/+}Rag2^{-/-}$ mice, the HLA-A-positive BMSCs were largely found at the trabecular bone surface and were RUNX2-negative at one week after injection. At two weeks after injection some of the injected human BMSCs at the trabecular bone surface in the $Tgfb1^{+/+}Rag2^{-/-}$ were RUNX2-positive. In contrast, the HLA-A-positive BMSCs were not found at the bone surfaces of the $Tgfb1^{-/-}Rag2^{-/-}$ mice at one week or two weeks after injection (Fig. 3i,j). Similar results were obtained (data not shown) when osteogenic $CD146^+CD45^-$ human BMSCs isolated by FACS (Supplementary Fig. 3a–c). Taken together, these results indicate that TGF-β1 is essential for the migration of BMSCs to the bone surfaces.

SMAD signaling mediates TGF-β1-induced migration of BMSCs

We then examined the signaling pathway(s) that mediates TGF-β1-induced migration of BMSCs. It is well established that phosphorylation of R-SMADs by TβRI is the primary TGF-β signaling pathway48,49. We found that a TβRI kinase-specific inhibitor (SB-505124)50 blocked the BRCM-induced migration of BMSCs in a concentration-dependent manner (Fig. 4a) and that retrovirus-mediated expression of SMAD7 inhibited the migration of the BMSCs (Fig. 4b), further indicating TGF-β1 acting through TβRI to induce migration of the BMSCs since SMAD7 is known to bind specifically to TβRI and inhibit phosphorylation of SMAD2/351. Moreover, retrovirus-mediated expression of a constitutively active TβRI in BMSCs was as effective in inducing the migration of the BMSCs as the addition of human natural TGF-β1 in a scratch assay (Supplementary Fig. 3d). Collectively, these data indicate that the TGF-β1-induced migration of BMSCs is mediated through TβRI signaling.

To examine the role of the TβRI downstream SMADs in TGF-β1-induced migration of BMSCs, we reduced the expression of endogenous SMAD2 or SMAD3 or both using siRNAs (Fig. 4c). Significant inhibition of BRCM-mediated cell migration was not observed on treatment with SMAD2 siRNA alone (Fig. 4c). Significant inhibition was observed when the cells were treated with SMAD3 siRNA alone and even greater inhibition was observed when the cells were treated with both siRNAs (Fig. 4c), suggesting that SMAD3 is primarily responsible for TGF-β1-induced migration of BMSCs and its function can be partially compensated by SMAD2. As the phosphorylated R-SMADs form a functional complex with SMAD4, the common signal transducer for all R-SMADs48, we also examined the effect of deletion of endogenous *Smad4* in primary mouse BMSCs on TGF-β1-induced cell migration. BMSCs isolated from *Smad4*$^{lox/lox}$ mice52 were infected with adenovirus bearing either Cre or GFP and the endogenous *Smad4* gene was deleted (Fig. 4d). BMSCs isolated from the mice with deletion of *Smad4* exhibited reduced BRCM-induced migration (Fig. 4d). Thus, SMAD signaling is essential for the TGF-β1-induced migration of BMSCs. During migration, cells exhibit characteristic lamellipodia-like protrusion structures that can be identified by staining with phalloidin. To examine the effects of SMAD signaling on the cytoskeleton, we used a model in which cell morphology can be examined as the BMSCs migrate towards a TGF-β1 gradient. The BMSCs exhibited directed migration within the TGF-β1 gradient (Supplementary Fig. 3e,f). In the absence of the gradient the cells exhibited low levels of random migration (Supplementary Fig. 3e,f). The BMSCs that were migrating towards the gradient exhibited typical lamellipodia-like protrusions (Supplementary Fig. 3g,h). Addition of the TβRI inhibitor was associated with a loss of formation of these protrusion structures although the formation of stress fibers was not affected. Similar results were obtained on deletion of *Smad4* in the primary BMSCs (Supplementary Fig. 3g,h), suggesting that the SMAD signaling pathway is required for the formation of the lamellipodia-like protrusions required for TGF-β1-induced cell migration. To examine the effect of interrupting TGF-β signaling and the TGF-β gradient on cell migration *in vivo*, GFP-labeled BMSCs were injected as described above with the TβRI inhibitor, active exogenous TGF-β1 or vehicle, and detected by immunostaining with GFP antibody. The BMSCs were largely found at the bone remodeling sites defined by the presence of TRAP-positive mature osteoclasts in the vehicle treatment group (Fig. 4e,f). Co-injection of TβRI inhibitor reduced the numbers of the BMSCs at the active remodeling surfaces (Fig. 4e,f). Moreover, co-injection of active exogenous TGF-β1 to interrupt the TGFβ1 gradient in bone also significantly reduced the BMSCs at the active remodeling surfaces (Fig. 4e,f). These results indicate that SMAD signaling mediates the TGF-β1-induced migration of BMSCs and interruption of TGF-β signaling and the TGF-β1 gradient reduces the recruitment of BMSCs to bone remodeling surfaces.

High active TGF-β1 in CED mice interrupts bone remodeling

To examine the effects of the CED *TGF-β1* point mutations of the *LAP* region on TGF-β1 activity, expression constructs of five *TGF-β1* point mutants identified in CED patients and the WT *TGF-β1* were generated and transfected into 293T cells. The conditioned media from cells expressing either mutant or WT *TGF-β1* contained the inactive latent form of TGF-β1; however, the conditioned media from the cells expressing mutant *TGF-β1* contained much higher levels of active TGF-β1 than the conditioned media of cells

expressing WT *TGF-β1* (Fig. 5a). We also found that the ratio of active to total TGF-β1 in the conditioned media from the cells expressing the mutant *TGF-β1* was significantly higher (Supplementary Fig. 4a) and that the conditioned media from the cells expressing mutant *TGF-β1* were hyperactive in inducing the migration of the human STRO-1^+ BMSCs (Fig. 5b). Thus, expression of the CED-derived *TGF-β1* mutants is associated with significantly enhanced formation of active TGF-β1.

To examine the effects of this enhanced formation of active TGF-β1 on bone formation, we generated two osteoblast tissue-specific transgenic mouse models, one with the CED-derived *TGF-β1* mutation (H222D) and one with WT *TGF-β1* as a control, in which the expression was driven by the 2.3 kb type I collagen promoter (Supplementary Fig. 4b). In both transgenic mice, two lines were obtained. The expression levels and their bone phenotypes were very similar between two founders of the same transgene. The specific expression of the CED mutant and WT *TGF-β1* in the bone tissue was confirmed (Supplementary Fig. 4c). Interestingly, the levels of total or latent TGF-β1 in the bone marrow were significantly higher in both CED and WT *TGF-β1* transgenic mice than in their WT littermates (Supplementary Fig. 4d,e), while the levels of active TGF-β1 in the bone marrow of CED mutant mice were much higher than in the WT *TGF-β1* transgenic mice or their WT littermates (Fig. 5c and Supplementary Fig. 4d), indicating premature release of active TGF-β1 in CED mice. There were no detectable defects in the skeleton of the neonatal CED mice (Fig. 5d). Diaphyseal thickening was initially observed as a characteristic of human CED explaining its alternative name progressive diaphyseal dysplasia. This typical thickening was observed in the lower limbs of one month-old CED mice (Fig. 5d,e). The major defects of the CED mice were found in the long bones. More than 50% of mice had tibial fractures by three months of age (Fig. 5d). Thus, enhanced formation of TGF-β1 in the bone marrow in these mice appears to be associated with defective bone remodeling that primarily affects the long bones.

The major bone defects in the long bones of the CED mice are similar to that seen in the CED patients. Such defects were not observed in either WT *TGF-β1* transgenic mice or the WT littermates although the total bone volumes did not differ among each of these genotypes (Fig. 5f,g). Consecutive measurements of cross-sectional bone volume along the length of the tibia by μCT demonstrated a fluctuating bone volume in the CED mice (Fig. 5h). Bone histomorphometric analysis of the tibia provided insights into the bases for this fluctuating bone volume. Similar to CED patients, the cortical thickness was increased about four folds relative to WT *TGF-β1* transgenic mice or littermates. The cortical bone porosity, osteoblasts surface, and osteoclasts surface were also significantly higher in CED mice, indicating high bone turnover and abnormal bone remodeling (Supplementary Table 1). Moreover, the osteoclasts and osteoblasts were clustered in separated areas (Fig. 5i), indicating uncoupled bone resorption and formation. Since the CED mutant *TGF-β1* was specifically expressed in the cells of ostoblastic lineages, the clustering of the osteoblasts is likely due to the high levels of active TGF-β1 secreted from the ostoblastic cells which may induce migration of BMSCs in this microenvironment and stimulate their proliferation. In parallel, the availability of BMSCs to bone resorptive sites is limited and osteoclastic bone resorption continued without bone formation during remodeling cycles. In addition, the

secretion of active TGF-β1 from the ostoblastic cells most likely blunts the TGF-β1 gradient created by osteoclastic bone resorption, as suggested by the ability of injection of exogenous TGF-β1 into the bone cavity to interfere with the recruitment of BMSCs to bone remodeling sites (Fig. 4e,f). Indeed, p-Smad2/3-positive cells were significantly more abundant in the areas of clustered osteoblasts in CED mice, indicating high levels of active TGF-β1. These effects were not seen in the WT *TGF-β1* transgenic mice (Supplementary Fig. 5a). On BrdU labeling, higher numbers of BrdU-labeled cells were observed in the CED mice (Supplementary Fig. 5b). Most importantly, the p-Smad2/3 and BrdU-positive cells were found in the vicinity of osteoclastic bone resorption surfaces in the WT *TGF-β1* transgenic mice or their littermates, whereas few of the p-Smad2/3 and BrdU-positive cells were found at the bone resorption sites in the CED mice (Supplementary Fig. 5a,b). These *in vivo* results indicated that secretion of high levels of active TGF-β1 by the osteoblastic cells in CED mice provided a microenvironment that resulted in the formation of clusters of osteoblastic cells and prohibited migration of the BMSCs to bone resorption sites.

TβRI inhibitor rescues bone remodeling defects in CED mice

If enhanced formation of active TGF-β1 in the bone marrow microenvironment uncouples bone resorption and formation in CED mice, inhibition of TGF-β1 activity in the bone marrow may be capable of preventing the bone remodeling defects in CED mice. To test this possibility, CED mice were injected intraperitoneally with different concentrations of TβRI inhibitor or vehicle every day for seven weeks. Analysis of long bone structures by X-ray and μCT revealed that injection of TβRI inhibitor resulted in an improvement in the bone morphology and the irregular distribution of bone mass and that these effects were dependent on the concentration of the injected TβRI inhibitor (Fig. 6a,b). Tibial fractures were largely prevented in CED mice, whereas more than 50% of fractures were still observed in the vehicle control group (Fig. 6a). Moreover, consecutive measurements of cross-sections of bone volume by μCT along the longitude of the tibia showed that the bone volume was more evenly distributed after TβRI inhibitor treatment (Fig. 6c), indicating the partial rescue of bone remodeling defects. Notably, the total bone volumes were not altered on treatment of the TβRI inhibitor (Fig. 6b and Supplementary Fig. 6a–c). The bone histomorphometric analysis showed that the CED mice treated with the TβRI inhibitor had significantly reduced cortical thickness, porosity, osteoblasts surface, and osteoclasts surface, indicating restoration of normal bone remodeling in CED mice (Supplementary Table 1).

Immunostaining of the tibial sections demonstrated that, in the CED mice treated with TβRI inhibitor, the osteocalcin-positive osteoblasts and TRAP-positive osteoclasts were associated on the bone surface. This was in marked contrast to the clustering of the osteoclastic cells and osteoblasts in separated areas in the vehicle-treated CED mice (Fig. 6d). Indeed, there was a reduction in the numbers of both p-Smad2/3 and BrdU-positive cells in the tibial sections of the CED mice treated with TβRI inhibitor, and these cells were dispersed and associated with TRAP-positive osteoclasts (Supplementary Fig. 6d,e). Inhibition of formation of osteoblastic cell clusters by the TβRI inhibitor may lead to a more even distribution of the BMSCs rendering them available to respond to osteoclastic bone resorption and thereby promoting the coupling of bone formation and resorption. Taken

together, these results indicate that uncoupled bone resorption and formation can be partially rescued by inhibiting abnormally high TGF-β1 activity in the bone microenvironment of CED mice.

DISCUSSION

The published data regarding the exact function of TGF-β1 in bone are seemingly ambiguous22. Although TGF-β1 has been shown to stimulate proliferation of progenitors and inhibit osteoblast differentiation of the osteoprogenitors in cell cultures and transgenic mouse models22, the skeleton of *Tgfb1*$^{-/-}$ mice appears to be normal at three weeks of age, and there are no reports of defects during prenatal skeletal development or perinatal bone growth in these mice44,45. Analysis of older *Tgfb1*$^{-/-}$ mice has been hindered by their early death due to the associated autoimmune disease43. The use of immunodeficient *Tgfb1*$^{-/-}$ *Rag2*$^{-/-}$ mice has allowed the analysis of older mice, and this has revealed that these mice do exhibit significant bone defects at three months of age. This implies that TGF-β1 does play a critical role in bone formation and further suggests that TGF-β1 plays a role in bone remodeling in adult mice.

TGF-β1-directed migration of BMSCs to the resorptive sites is an essential step in the coupling process. The BMSCs then undergo osteoblastic differentiation in response to the signals provided by the microenvironment of the resorptive sites. To track the migration of osteogenic BMSCs *in vivo*, we used both human osteogenic BMSCs sorted by STRO-1 or CD146 and mouse osteogenic BMSCs sorted by Sca-1, CD29, CD45 and CD11b as there is no unique marker for osteogenic BMSCs. We found that TGF-β1-induced migration of BMSCs to the bone surfaces where osteoblast differentiation was induced. Both the physical properties of the fresh resorption site and soluble factors likely contribute to the differentiation of BMSCs. At fresh resorptive sites, the bone mineral matrix is exposed and lacks a covering of lining cells, providing a stiff elastic microenvironment that can direct differentiation of BMSCs53. The exposed bone is also rich in osteotropic factors, including BMPs, IGF-I, IGF-II and PDGF, which promote osteoblastic differentiation of BMSCs into osteoblasts. In the absence of directed migration and attachment to the freshly exposed bone remodeling surface, the BMSCs are unlikely to differentiate into osteoblasts effectively. This may contribute, in part, to bone loss at the sites of resorption specifically and, perhaps, a more generalized bone loss in the *Tgfb1*$^{-/-}$ mice.

Alterations in bone remodeling are often associated with bone diseases, including CED, hyperparathyroidism, Paget's disease, multiple myeloma, osteoporosis and osteopetrosis3. The association of point mutations of the *TGF-β1 LAP* region with CED provides an ideal *in vivo* model to validate the role of TGF-β1 in coupling bone resorption and formation. Introduction of a CED *TGF-β1* point mutation resulted in significant bone remodeling defects in these transgenic mice although their total bone volumes did not differ significantly from that of their WT littermates. The levels of total and latent TGF-β1 were high in both the CED and WT *TGF-β1* transgenic mice; whereas the CED mice differed from their WT littermates and WT control transgenic mice in that they expressed high levels of active TGF-β1 in the bone marrow microenvironment. These *in vivo* observations provide further

evidence that active TGF-β1 plays a primary role in coupling bone resorption and formation in adult mice.

The currently available strategies for the treatment of osteoporosis are basedon either specific inhibition of osteoclast activity or stimulation of osteoblast activity and their effectiveness is compromised by the attempts of the internal coupling mechanism to balance bone resorption and formation3. Our results suggest novel approaches for anti-osteoporosis therapy based on direct targeting of the balance between bone resorption and formation. The adult skeleton undergoes constant remodeling and many diseases of the bone are associated with defects in the coupling process. In primary hyperparathyroidism, hyperthyroidism and Paget's disease, there is excess bone formation after each cycle of osteclastic bone resorption during remodeling54–56. Our results suggest that targeting of TGFβ1 signaling could potentially prove to be an effective therapy for these disorders.

METHODS

Animals

We obtained *Tgfb1*$^{+/-}$*Rag2*$^{-/-}$ mice from MMHCC Repository Laboratory Animal Sciences Program, NCI as described previously47. *Tgfb1*$^{+/-}$*Rag2*$^{-/-}$ mice were maintained as heterozygotes and were crossed to generate *Tgfb1*$^{-/-}$*Rag2*$^{-/-}$, *and Tgfb1*$^{+/+}$*Rag2*$^{-/-}$ mice. *Smad4* floxed mice were generously provided by Dr. Chuxia Deng52. To establish a mouse model with a CED-derived *TGF-β1* mutation, a 1.1 kb *Eco*RI-*Sma*I cDNA fragment containing the full-length *TGF-β1* with a point mutation (H222D) was ligated into a vector with a bone-specific expression promoter of type I collagen (Col1A1 2.3 kb). Full-length wild type *TGF-β1* (WT) was also ligated into the same vector. DNA fragments composed of *Col1A1*, the insert and *SV40* were released from the vector with digestion of *Xho*I and *Sap*I unique restriction sites at the 5′ and 3′ ends of the transgene. The two transgenic DNA fragments were microinjected into mouse C57BL/J6 eggs and surgically transferred to recipients by standard techniques respectively. All animals were maintained in the Animal Facility of the University of Alabama at Birmingham School of Medicine. The experimental protocol was reviewed and approved by the Institutional Animal Care and Use Committee (IACUC) of the University of Alabama at Birmingham, Birmingham, AL, USA.

Purification and characterization of human and mouse BMSCs

BMSCs were defined by the International Society for Cellular Therapy. We obtained human bone marrow from the UAB Bone Cell Core Facility based on a protocol approved by the UAB Institutional Review Board. The plastic adherent human BMSCs were isolated by immunoselection using the mouse antibody to STRO-1 (dilution: 0.1 mg ml^{-1} and 10 μl of the diluted solution to 1–2.5 × 10^5 cells in a total reaction volume) and rat anti-mouse IgM-conjugated magnetic beads (Dynatech) according to the manufacturer's directions (for *in vitro* migration assay). The adherent human BMSCs also were sorted by fluorescence-activated cell sorting (FACS) with the antibodies to CD45 (Bio-legend Inc) and CD146 (Abcam Inc) to harvest CD146$^+$CD45$^-$ BMSCs. Mouse bone marrow cells were harvested and cultured. The adherent cells57–59 were further sorted by FACS using the antibodies to CD29, Sca-1, CD45 and CD11b (Bio-legend Inc). The sorted cells were enriched by further

culture and confirmed by flow cytometry. Colony forming unit-fibroblast (CFU-F)57,59 was analyzed by culturing 5×10^3 sorted cells to T-25 flask. The CFU-F colonies were further induced with osteogenic medium for seven days and analyzed with AP staining. The BMSCs cells were also cultured with or without osteogenic medium for 21 days for von Kossa or Alizarin Red staining.

Bone marrow cavity transplantation of BMSCs

We used age-matched *Tgfb1*$^{-/-}$ or wild-type littermates with an immuno-deficient background (*Tgfb1*$^{-/-}$ *Rag2*$^{-/-}$ and *Tgfb1*$^{+/+}$*Rag2*$^{-/-}$ mice, male, three months) as recipients. The mice (five in each group) were anesthetized by inhalation of isoflurane, and the left distal femur was gently drilled with a 26 G needle through the patellar tendon. The GFP-labeled mouse BMSCs or human BMSCs (1×10^6) in 10 μl of α-MEM were injected into the bone cavity through the hole in the femur using a microsyringe. To interrupt TGF-β1 signaling and gradient *in vivo*, the donor GFP-labeled BMSCs were transplanted together with either TGF-β type I receptor (TβRI) inhibitor (Sigma-Aldrich Inc, SB-505124, 100 nM) or TGF-β1 (Sigma-Aldrich Inc, 20 ng, before use, the product was treated with 4 mM HCL containing 1 mg ml^{-1} BSA to make a stock solution and activate the protein) or vehicle into the bone cavity. The mice were sacrificed at different time after transplantation and the distal femurs were resected and stained.

Generation of *TGF-β1* mutant constructs and transfection in cells

We cloned the human cDNA of *TGF-β1* into pCDNA3 vector. The point mutations (R156C, R218C, H222D, C223R or C225R) in the latency-associated peptide of *TGF-β1* were generated by site-directed mutagenesis using the Quik-Change® Site-Directed Mutagenesis Kit (Stratagene) according to the manufacturer's protocol. For transient expression of the mutant and WT *TGF-β1* gene products, HEK-293T cells were transfected with each of the constructs and 10 ng of the internal control pRL-0 vector (Promega) by Lipofectamine (Gibco-BRL). Cultured media or cell lysates were collected after transfection for detection of protein expression by ELISAs and Western blots.

Statistical analyses

Data were analyzed using an ANOVA or Student's *t*- test and are presented as the mean ± SEM. We considered a *P* value < 0.05 significant.

Supplementary Material

Refer to Web version on PubMed Central for supplementary material.

Acknowledgments

The authors thank F. Hunter and T. Clemens for their critical review and discussion for the manuscript; H.L. Moses, C. Deng, J. Murphy-Ullrich and W. Xiong for reagents. This research was supported by National Institutes of Health grant AR 053973 and DK057501. We thank the UAB Center for Metabolic Bone Disease Cores for small animal phenotyping, histomorphometry and molecular analyses.

References

1. Teitelbaum SL. Bone resorption by osteoclasts. Science. 2000; 289:1504–1508. [PubMed: 10968780]
2. Abe E, et al. TSH is a negative regulator of skeletal remodeling. Cell. 2003; 115:151–162. [PubMed: 14567913]
3. Zaidi M. Skeletal remodeling in health and disease. Nature Medicine. 2007; 13:791–801.
4. Hill PA. Bone remodelling. Br J Orthod. 1998; 25:101–107. [PubMed: 9668992]
5. Janssens K, et al. Mutations in the gene encoding the latency-associated peptide of TGF-beta 1 cause Camurati-Engelmann disease. Nature Genetics. 2000; 26:273–275. [PubMed: 11062463]
6. Kinoshita A, et al. Domain-specific mutations in the human transforming growth factor beta 1 gene (TGFB1) result in Camurati-Engelmann disease. American Journal of Human Genetics. 2000; 67:370.
7. Hecht JT, et al. Evidence for locus heterogeneity in the Camurati-Engelmann (DPD1) Syndrome. Clinical Genetics. 2001; 59:198–200. [PubMed: 11260231]
8. Oreffo RO, Mundy GR, Seyedin SM, Bonewald LF. Activation of the bone-derived latent TGF beta complex by isolated osteoclasts. Biochem Biophys Res Commun. 1989; 158:817–823. [PubMed: 2920041]
9. Mundy GR. Peptides and growth regulatory factors in bone. Rheum Dis Clin North Am. 1994; 20:577–588. [PubMed: 7984779]
10. Martin TJ, Allan EH, Fukumoto S. The Plasminogen-Activator and Inhibitor System in Bone Remodeling. Growth Regulation. 1993; 3:209–214. [PubMed: 8130729]
11. Hill PA, Tumber A, Meikle MC. Multiple extracellular signals promote osteoblast survival and apoptosis. Endocrinology. 1997; 138:3849–3858. [PubMed: 9275074]
12. Pfeilschifter J, et al. Chemotactic Response of Osteoblast-Like Cells to Transforming Growth-Factor-Beta. Journal of Bone and Mineral Research. 1990; 5:825–830. [PubMed: 2239366]
13. Linkhart TA, Mohan S, Baylink DJ. Growth factors for bone growth and repair: IGF, TGF beta and BMP. Bone. 1996; 19:S1–S12.
14. Hughes FJ, Aubin JE, Heersche JNM. Differential Chemotactic Responses of Different Populations of Fetal-Rat Calvaria Cells to Platelet-Derived Growth-Factor and Transforming Growth-Factor-Beta. Bone and Mineral. 1992; 19:63–74. [PubMed: 1422306]
15. Bismar H, et al. Transforming growth factor beta (TGF-beta) levels in the conditioned media of human bone cells: relationship to donor age, bone volume, and concentration of TGF-beta in human bone matrix in vivo. Bone. 1999; 24:565–569. [PubMed: 10375198]
16. Roberts AB, Frolik CA, Anzano MA, Sporn MB. Transforming growth factors from neoplastic and nonneoplastic tissues. Fed Proc. 1983; 42:2621–2626. [PubMed: 6303865]
17. Seyedin SM, Thomas TC, Thompson AY, Rosen DM, Piez KA. Purification and characterization of two cartilage-inducing factors from bovine demineralized bone. Proc Natl Acad Sci U S A. 1985; 82:2267–2271. [PubMed: 3857579]
18. Dallas SL, et al. Characterization and Autoregulation of Latent Transforming Growth-Factor-Beta (Tgf-Beta) Complexes in Osteoblast-Like Cell-Lines - Production of A Latent Complex Lacking the Latent Tgf-Beta-Binding Protein. Journal of Biological Chemistry. 1994; 269:6815–6822. [PubMed: 8120044]
19. Gentry LE, Lioubin MN, Purchio AF, Marquardt H. Molecular events in the processing of recombinant type 1 pre-pro-transforming growth factor beta to the mature polypeptide. Mol Cell Biol. 1988; 8:4162–4168. [PubMed: 3185545]
20. Pfeilschifter J, Bonewald L, Mundy GR. Characterization of the latent transforming growth factor beta complex in bone. J Bone Miner Res. 1990; 5:49–58. [PubMed: 2309578]
21. Pedrozo HA, et al. Potential mechanisms for the plasmin-mediated release and activation of latent transforming growth factor-beta 1 from the extracellular matrix of growth plate chondrocytes. Endocrinology. 1999; 140:5806–5816. [PubMed: 10579347]
22. Janssens K, ten Dijke P, Janssens S, Van Hul W. Transforming growth factor-beta 1 to the bone. Endocrine Reviews. 2005; 26:743–774. [PubMed: 15901668]

23. Jian HY, et al. Smad3-dependent nuclear translocation of beta-catenin is required for TGF-beta 1-induced proliferation of bone marrow-derived adult human mesenchymal stem cells. Genes & Development. 2006; 20:666–674. [PubMed: 16543220]
24. Erlebacher A, Filvaroff EH, Ye JQ, Derynck R. Osteoblastic responses to TGF-beta during bone remodeling. Molecular Biology of the Cell. 1998; 9:1903–1918. [PubMed: 9658179]
25. Filvaroff E, et al. Inhibition of TGF-beta receptor signaling in osteoblasts leads to decreased bone remodeling and increased trabecular bone mass. Development. 1999; 126:4267–4279. [PubMed: 10477295]
26. Janssens K, et al. Camurati-Engelmann disease: review of the clinical, radiological, and molecular data of 24 families and implications for diagnosis and treatment. Journal of Medical Genetics. 2006; 43:1–11. [PubMed: 15894597]
27. Janssens K, ten Dijke P, Ralston SH, Bergmann C, Van Hul W. Transforming growth factor-beta 1 mutations in Camurati-Engelmann disease lead to increased signaling by altering either activation or secretion of the mutant protein. Journal of Biological Chemistry. 2003; 278:7718–7724. [PubMed: 12493741]
28. Saito T, et al. Domain-specific mutations of a transforming growth factor (TGF)-beta 1 latency-associated peptide cause Camurati-Engelmann disease because of the formation of a constitutively active form of TGF-beta 1. Journal of Biological Chemistry. 2001; 276:11469–11472. [PubMed: 11278244]
29. Prockop DJ. Marrow stromal cells as stem cells for nonhematopoietic tissues. Science. 1997; 276:71–74. [PubMed: 9082988]
30. Caplan AI. Mesenchymal Stem-Cells. Journal of Orthopaedic Research. 1991; 9:641–650. [PubMed: 1870029]
31. Dennis JE, Carbillet JP, Caplan AI, Charbord P. The STRO-1+marrow cell population is multipotential. Cells Tissues Organs. 2002; 170:73–82. [PubMed: 11731697]
32. Gronthos S, Graves SE, Ohta S, Simmons PJ. The Stro-1(+) Fraction of Adult Human Bone-Marrow Contains the Osteogenic Precursors. Blood. 1994; 84:4164–4173. [PubMed: 7994030]
33. Sacchetti B, et al. Self-renewing osteoprogenitors in bone marrow sinusoids can organize a hematopoietic microenvironment. Cell. 2007; 131:324–336. [PubMed: 17956733]
34. Meirelles LD, Nardi NB. Murine marrow-derived mesenchymal stem cell: isolation, in vitro expansion, and characterization. British Journal of Haematology. 2003; 123:702–711. [PubMed: 14616976]
35. Leucht P, et al. Effect of mechanical stimuli on skeletal regeneration around implants. Bone. 2007; 40:919–930. [PubMed: 17175211]
36. Caplan AI. Mesenchymal stem cells: Cell-based reconstructive therapy in orthopedics. Tissue Engineering. 2005; 11:1198–1211. [PubMed: 16144456]
37. Horwitz EM, et al. Transplantability and therapeutic effects of bone marrow-derived mesenchymal cells in children with osteogenesis imperfecta. Nature Medicine. 1999; 5:309–313.
38. Horwitz EM, et al. Isolated allogeneic bone marrow-derived mesenchymal cells engraft and stimulate growth in children with osteogenesis imperfecta: Implications for cell therapy of bone. Proceedings of the National Academy of Sciences of the United States of America. 2002; 99:8932–8937. [PubMed: 12084934]
39. Mirmalek-Sani SH, et al. Characterization and multipotentiality of human fetal femur-derived cells: Implications for skeletal tissue regeneration. Stem Cells. 2006; 24:1042–1053. [PubMed: 16373694]
40. Canalis E, Economides AN, Gazzerro E. Bone morphogenetic proteins, their antagonists, and the skeleton. Endocrine Reviews. 2003; 24:218–235. [PubMed: 12700180]
41. Ozaki Y, et al. Comprehensive analysis of chemotactic factors for bone marrow mesenchymal stem cells. Stem Cells and Development. 2007; 16:119–129. [PubMed: 17348810]
42. Maeda S, Hayashi M, Komiya S, Imamura T, Miyazono K. Endogenous TGF-beta signaling suppresses maturation of osteoblastic mesenchymal cells. Embo Journal. 2004; 23:552–563. [PubMed: 14749725]

43. Kulkarni AB, et al. Transforming Growth Factor-Beta-1 Null Mutation in Mice Causes Excessive Inflammatory Response and Early Death. Proceedings of the National Academy of Sciences of the United States of America. 1993; 90:770–774. [PubMed: 8421714]
44. Geiser AG, et al. Decreased bone mass and bone elasticity in mice lacking the transforming growth factor-beta 1 gene. Bone. 1998; 23:87–93. [PubMed: 9701466]
45. Atti E, et al. Effects of transforming growth factor-beta deficiency on bone development: a Fourier transform-infrared imaging analysis. Bone. 2002; 31:675–684. [PubMed: 12531561]
46. Shinkai Y, et al. Rag-2-Deficient Mice Lack Mature Lymphocytes Owing to Inability to Initiate V(D)J Rearrangement. Cell. 1992; 68:855–867. [PubMed: 1547487]
47. Engle SJ, et al. Elimination of colon cancer in germ-free transforming growth factor beta 1-deficient mice. Cancer Research. 2002; 62:6362–6366. [PubMed: 12438215]
48. Massague J. TGF-beta signal transduction. Annual Review of Biochemistry. 1998; 67:753–791.
49. Attisano L, Wrana JL. Signal transduction by the TGF-beta superfamily. Science. 2002; 296:1646–1647. [PubMed: 12040180]
50. DaCosta BS, Major C, Laping NJ, Roberts AB. SB-505124 is a selective inhibitor of transforming growth factor-beta type I receptors ALK4, ALK5, and ALK7. Mol Pharmacol. 2004; 65:744–752. [PubMed: 14978253]
51. Hayashi H, et al. The MAD-related protein Smad7 associates with the TGF beta receptor and functions as an antagonist of TGF beta signaling. Cell. 1997; 89:1165–1173. [PubMed: 9215638]
52. Yang X, Li CL, Herrera PL, Deng CX. Generation of Smad4/Dpc4 conditional knockout mice. Genesis. 2002; 32:80–81. [PubMed: 11857783]
53. Engler AJ, Sen S, Sweeney HL, Discher DE. Matrix elasticity directs stem cell lineage specification. Cell. 2006; 126:677–689. [PubMed: 16923388]
54. Zink AR, et al. Evidence for a 7000-year-old case of primary hyperparathyroidism. Jama-Journal of the American Medical Association. 2005; 293:40–42.
55. Roodman GD, Windle JJ. Paget disease of bone. Journal of Clinical Investigation. 2005; 115:200–208. [PubMed: 15690073]
56. Surks MI, et al. Subclinical thyroid disease - Scientific review and guidelines for diagnosis and management. Jama-Journal of the American Medical Association. 2004; 291:228–238.
57. Friedenstein AJ, Chailakhyan RK, Gerasimov UV. Bone marrow osteogenic stem cells: in vitro cultivation and transplantation in diffusion chambers. Cell Tissue Kinet. 1987; 20:263–272. [PubMed: 3690622]
58. Owen M, Friedenstein AJ. Stromal stem cells: marrow-derived osteogenic precursors. Ciba Found Symp. 1988; 136:42–60. [PubMed: 3068016]
59. Friedenstein AJ, et al. Precursors for fibroblasts in different populations of hematopoietic cells as detected by the in vitro colony assay method. Exp Hematol. 1974; 2:83–92. [PubMed: 4455512]

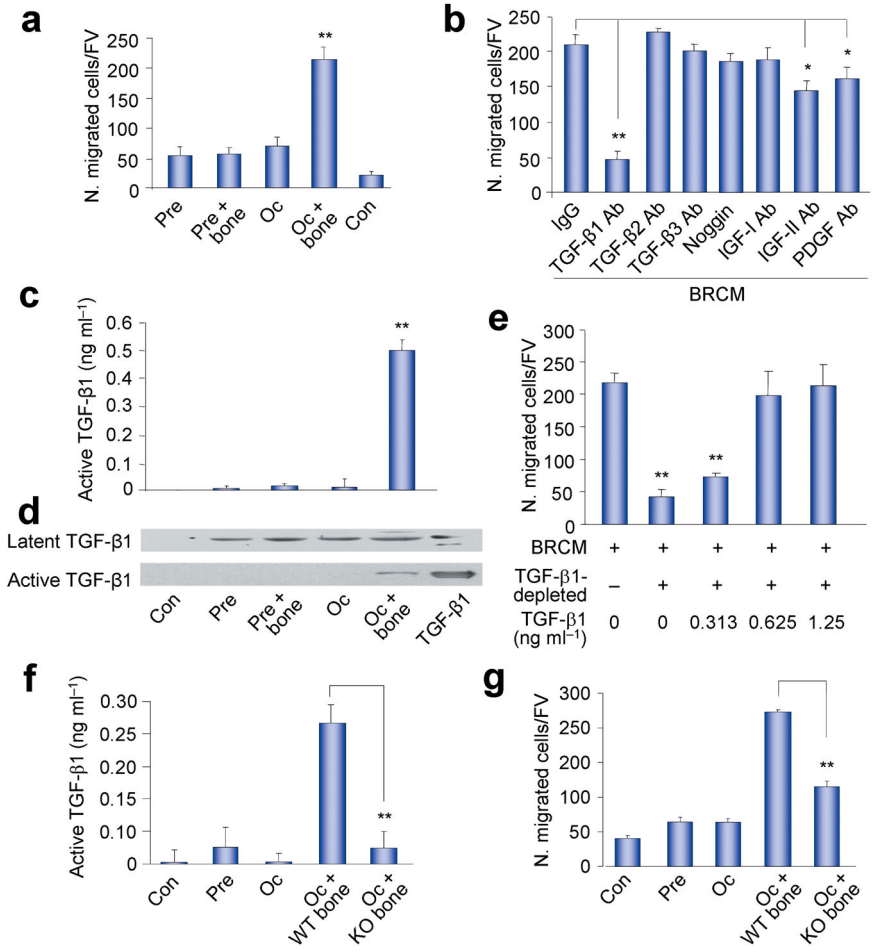

Figure 1.

Osteoclastic bone resorption-conditioned medium (BRCM) induces migration of BMSCs. (**a**) Transwell assays for migration of human STRO-1$^+$ BMSCs using BRCM harvested from different cell cultures (Pre, osteoclast precursors culture; Pre + bone, Osteoclast precursors cultured with bone slice; Oc, Osteoclasts culture; Oc + bone, Osteoclasts cultured with bone; Con, Control medium). N. migrated cells/FV, number of migrated cells per field of view. $n = 3$. $^{**}P < 0.01$, Oc + bone versus other groups. (**b**) Transwell assays for the migration of human STRO-1$^+$ BMSCs using BRCM with addition of individual neutralizing antibodies or noggin as indicated. Ab, antibody. $n = 3$. $^{*}P < 0.05$, $^{**}P < 0.01$. (**c,d**) ELISA (**c**) and Western blot (**d**) assays of TGF-β1 in BRCM. $n = 3$. $^{**}P < 0.01$, Oc + bone versus other groups, human natural TGF-β1 protein used as a positive control. (**e**) Addition of human natural TGF-β1 protein to the TGF-β1-depleted BRCM rescued the induction of migration. $n = 3$. $^{**}P < 0.01$ versus BRCM alone. (**f,g**) Active TGF-β1 detected by ELISA in BRCM prepared from osteoclast precursors or osteoclasts with bone slices of either *Tgfb1*$^{+/-}$ mice (KO bone) or their wild-type littermates (WT bone) (**f**), and Transwell migration analysis of human STRO-1$^+$ BMSCs induce by these BRCM (**g**). $n = 3$. $^{**}P < 0.01$.

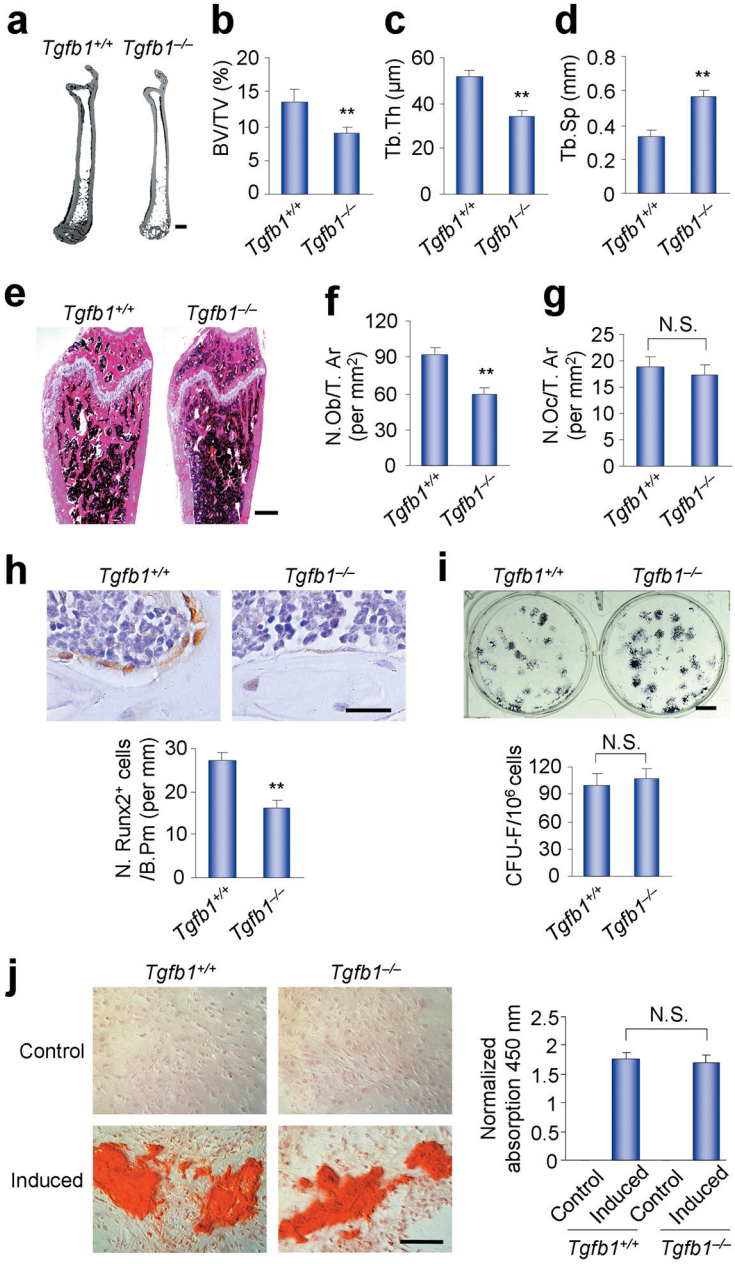

Figure 2.

Tgfb1$^{-/-}$*Rag2*$^{-/-}$ mice show decreased bone mass. (**a**) Representative images of three dimensional micro-computed tomography (μCT) of the whole right femora from three month-old *Tgfb1*$^{+/+}$*Rag2*$^{-/-}$ *and Tgfb1*$^{-/-}$*Rag2*$^{-/-}$ mice. Scale bar, 2 mm. (**b–d**) Structure parameters, including bone volume fraction (BV/TV, **b**), trabecular thickness (Tb. Th, **c**) and trabecular separation (Tb. Sp, **d**) as measured by μCT. $n = 5$. $^{**}P < 0.01$. (**e**) Images of histological sections of three month-old mouse femora stained by HE. Scale bar, 1 mm. (**f**,**g**) Bone histomorphometric analysis in the femora of three month-old mice. Number of osteoblasts per tissue area (N. Ob/T. Ar) (**f**) and number of osteoclasts per tissue area (N. Oc/T. Ar) (**g**) were measured. n=5. $^{**}P < 0.01$. N. S., not significant. (**h**) Immunostaining of

Runx2 positive cells in three month-old *Tgfb1*$^{+/+}$*Rag2*$^{-/-}$ and *Tgfb1*$^{-/-}$*Rag2*$^{-/-}$ mice. Scale bar, 25 μm. n=5. **P < 0.01. (**i,j**) CFU-F formation and alkaline phosphates (AP) staining after osteogenic medium induction in BMSCs harvested from three month-old *Tgfb1*$^{+/+}$*Rag2*$^{-/-}$ and *Tgfb1*$^{-/-}$*Rag2*$^{-/-}$mice (**i**). Scale bar, 0.5 cm. n = 3. N. S., not significant. These BMSCs were also stained with Alizarin Red after 21 days of induction with or without osteogenic medium, and the amount of Alizarin Red staining was measured by the absorption of 450 nm (**j**). Scale bar, 50 μm. n = 3. N. S., not significant.

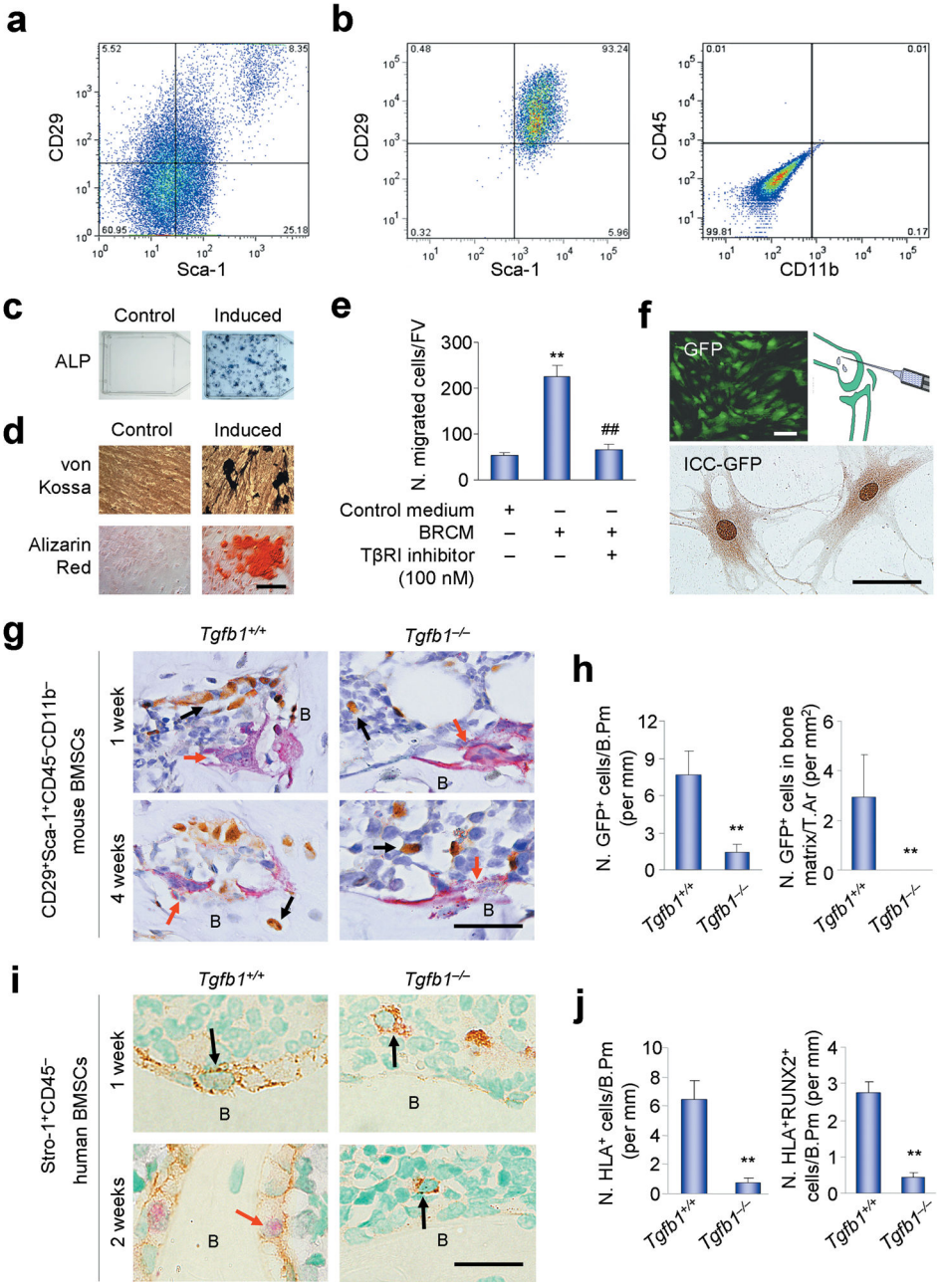

Figure 3.

Migration of the implanted BMSCs to bone resportive sites decreases in *Tgfb1*$^{-/-}$ mice. (**a**) FACS of CD29^{+}Sca-1^{+}CD45^{-}CD11b^{-} BMSCs. (**b**) Flow cytometry of the sorted cells. (**c**) CFU-F formation and AP staining of the sorted cells induced with or without osteogenic medium. (**d**) von Kossa and Alizarin Red staining of the sorted cells induced with or without osteogenic medium for 21 days. (**e**) Migration of the sorted cells induced by BRCM, with or without TβRI inhibitor (SB-505124) treatment. $n = 3$. $^{**}P < 0.01$ versus Control medium, $^{\#\#}P < 0.01$ versus BRCM without TβR1 inhibitor. (**f**) The sorted cells infected with GFP-retrovirus (left panel) were confirmed by immunocytochemisty staining (ICC) for GFP

expression (bottom panel), and were transplanted to mouse femur marrow cavity (right panel). (**g**) Images of the femur sections from three month-old mice transplanted with GFP-labeled mouse BMSCs co-stained with TRAP and the antibody to GFP. Red arrows indicate TRAP positive osteoclasts. Black arrows indicate GFP positive donor cells. B, bone. (**h**) Counts of GFP positive cells on bone surface one week after transplantation (N. GFP^+ cells/B. Pm: Number of GFP positive cells on bone surface) or in bone matrix four weeks after transplantation (N. GFP^+ cells/T. Ar: Number of GFP positive cells in bone tissue area). $n = 5$. $^{**}P < 0.01$. (**i,j**) Images (**i**) and counts (**j**) of human $STRO\text{-}1^+CD45^-$BMSCs transplanted into mouse femur cavities detected by antibodies to HLA-A and RUNX2. $n = 5$. $^{**}P < 0.01$. Scale bars, 25 μm.

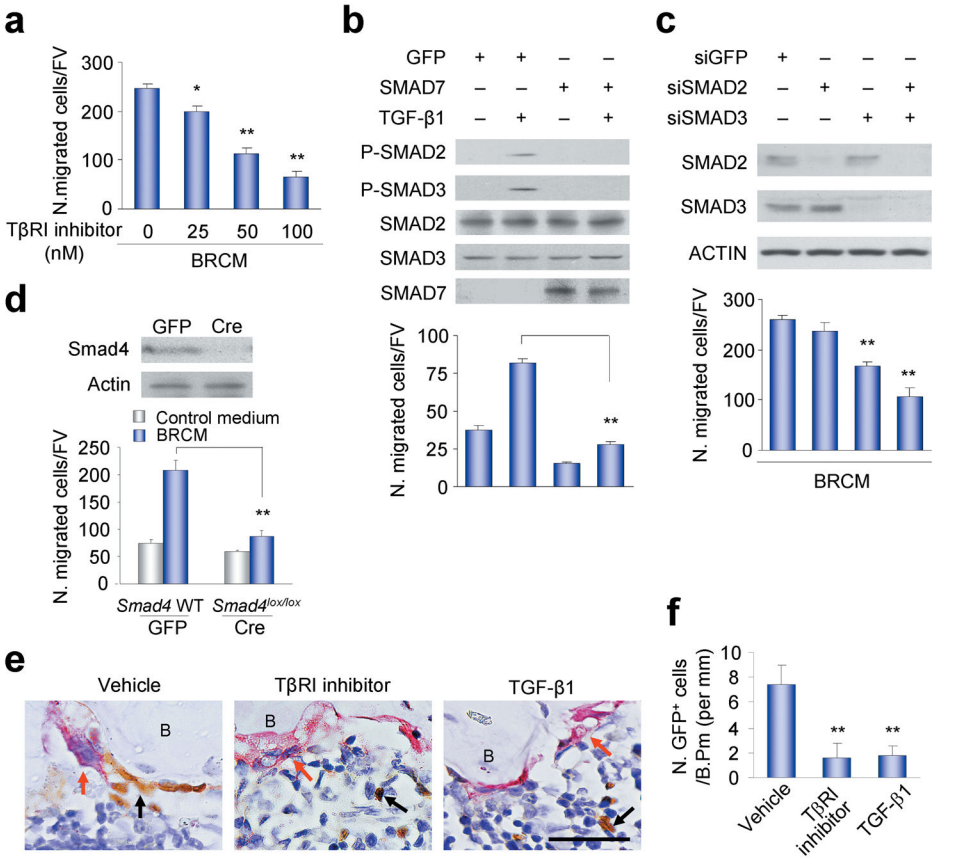

Figure 4.

SMAD signaling pathway mediates TGF-β1-induced migration of BMSCs. (**a**) Migration of human STRO-1$^+$ BMSCs treated with or without TβRI inhibitor (SB-505124). $n = 3$. *$P < 0.05$, **$P < 0.01$ versus TβR1 inhibitor 0 nM. (**b**) Phosphorylation of SMAD2/3 (p-SMAD2/3) and cell migration induced by TGFβ1 in the BMSCs expressing GFP or SMAD7. $n = 3$. **$P < 0.01$. (**c**) BRCM-induced migration of the human STRO-1$^+$ BMSCs transfected with siRNAs. Western blots of SMADs and ACTIN in these human STRO-1$^+$ BMSCs indicted in the upper panels. $n = 4$. **$P < 0.01$ versus siGFP group. (**d**) Migration of *Smad4*-deleted primary mouse BMSCs induced by BRCM. Western bolts of Smad4 and Actin in these mouse BMSCs indicated in the upper panels. $n = 3$. **$P < 0.01$. (**e,f**) Interruption of TGF-β1 signaling *in vivo* inhibited the migration of BMSCs. The GFP-labeled mouse BMSCs sorted by FACS were transplanted together with TβRI inhibitor (SB-505124), human natural TGF-β1 or vehicle into *Tgfb1*$^{+/+}$*Rag2*$^{-/-}$mice, and the sections were detected with TRAP staining and immunostaining for GFP (**e**). Red arrows indicate TRAP positive osteoclasts. Black arrows indicate GFP positive donor cells. Scale bar, 25 μM. B, bone. Counts of GFP positive cells on bone surface (N. GFP$^+$ cells/B. Pm) were shown in (**f**). $n = 5$. **$P < 0.01$ versus vehicle.

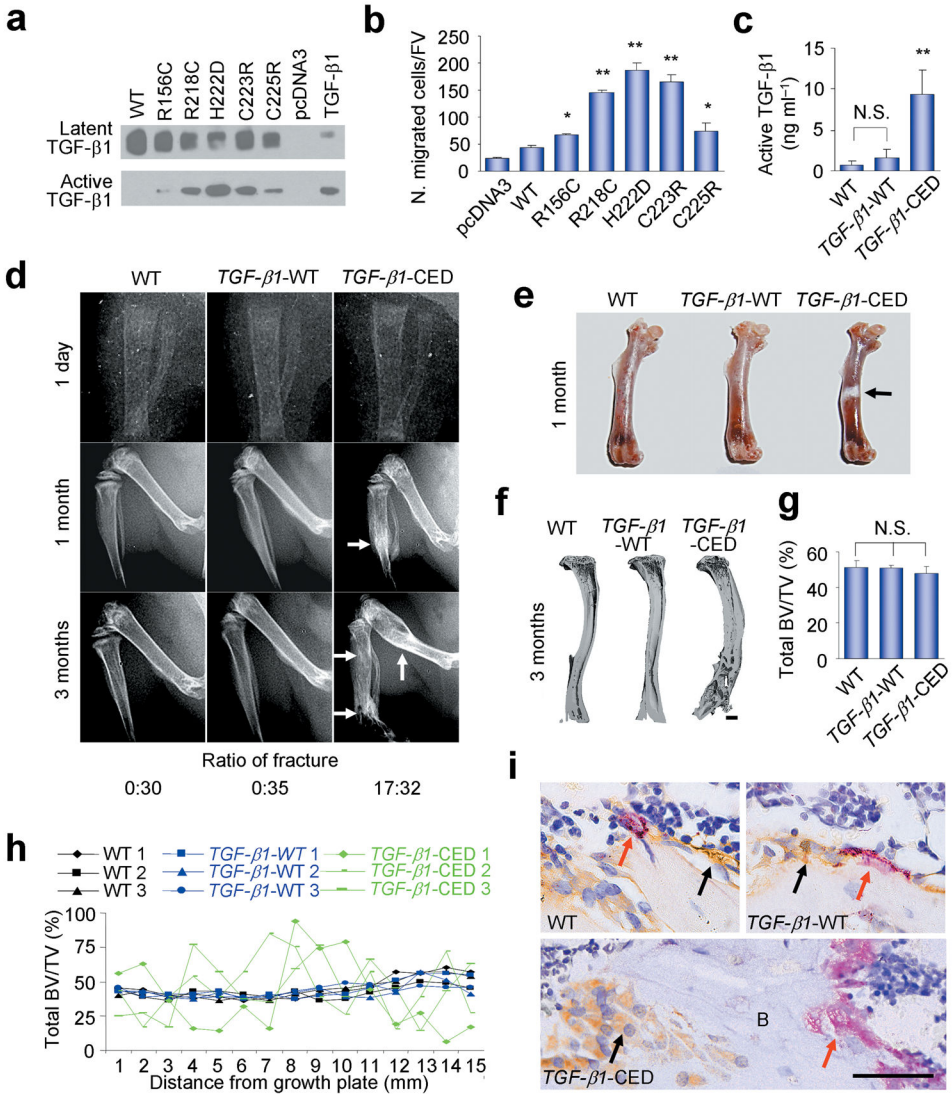

Figure 5.

Bone resorption is uncoupled with bone formation in CED transgenic mice. (**a**) The protein levels of latent and active TGF-β1 in conditioned medium prepared from HEK-293 cells transfected with WT *TGF-β1* or CED *TGF-β1* mutant expression plasmids, human natural TGFβ1 loaded as a positive control. (**b**) Conditioned medium prepared in (**a**) induces migration of human STRO-1$^+$ BMSCs. $n = 3$. *$P < 0.05$; **$P < 0.01$ versus WT. (**c**) The amount of active TGF-β1 in the bone marrow was measured by ELISA. $n = 10$. **$P < 0.01$ versus WT. N. S., not significant. (**d**) Radiography of right lower limbs of WT, *TGF-β1*-WT, and *TGF-β1*-CED mice at different ages. Arrows indicate the progressive diaphyseal dysplasia in *TGF-β1*-CED mice. Ratio of number of mice with fractures to total number of mice was counted. (**e**) Right femora images of one month-old male WT, *TGF-β1*-WT, and *TGF-β1*-CED mice. Arrow indicates diaphyseal dysplasia in *TGF-β1*-CED mice. (**f**) Three dimensional images of μCT from whole right tibiae of WT, *TGF-β1*-WT, and *TGF-β1*-CED mice. Scale bar, 2 mm. (**g**) Quantitative μCT image analysis of the whole tibiae. Total

BV/TV: total bone volume of tibia per tissue volume. *n* = 10. N. S., not significant. (**h**) Continuous scanning of total BV/TV (0.5 mm width) of tibiae cross section by μCT as the distance from growth plate. (**i**) Tibiae sections of three month-old WT, *TGF-β1*-WT, and *TGF-β1*-CED mice were stained with antibody to osteocalcin (black arrows) and with TRAP staining (red arrows). B, bone. Scale bar, 25 μm.

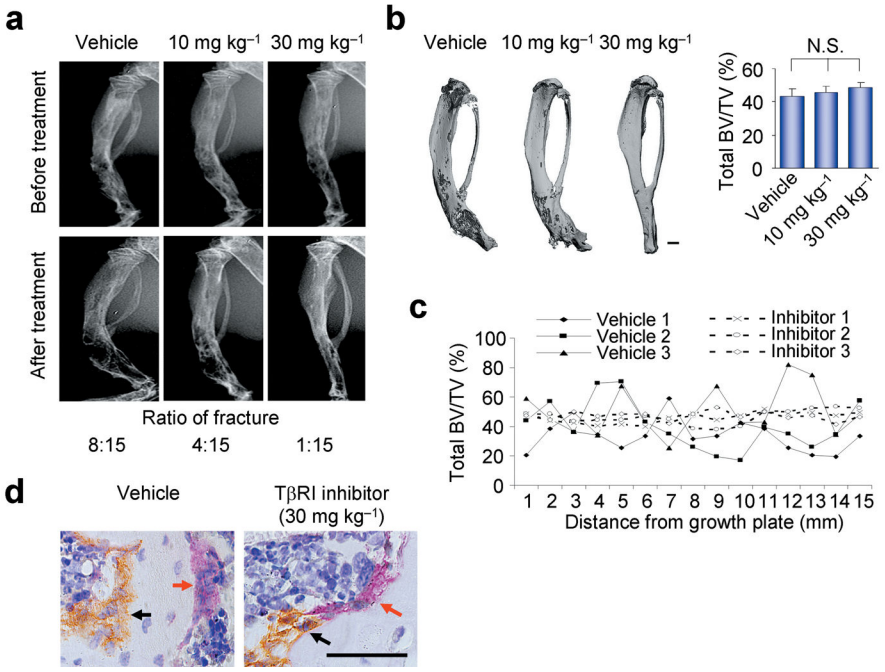

Figure 6.

TβRI inhibitor partially rescues uncoupled bone remodeling in *TGF-β1*-CED mice. Two month-old male *TGF-β1*-CED mice without fractures were injected intraperitoneally with either vehicle or SB-505124, a TβRI inhibitor, at different dosages (10 or 30 mg kg^{-1}) each day for seven weeks. (**a**) Radiography of right tibiae of mice before and after treatment from the indicated treatment groups. Ratio of number of mice with fractures to total number of mice after treatment was counted. (**b**) Tree dimensional μCT images and total BV/TV of tibiae from the indicated treatment groups. Scale bar, 2 mm. *n* = 15. N. S., not significant. (**c**) Continuous scanning of total BV/TV (0.5 mm width) of tibia cross section by μCT shown as the distance from growth plate. Three individual mice in *TGF-β1*-CED with vehicle (vehicle 1–3) and SB-505124 30 mg kg^{-1} (Inhibitor 1–3) treatment groups are presented respectively. (**d**) Tibiae sections from the indicated treatment groups were stained with antibody to osteocalcin for osteoblasts (black arrows) and with TRAP staining for osteoclasts (red arrows). Scale bar, 25 μm.